Peremennye Zvezdy (*Variable Stars*) **46**, No. 4, 2026

Received 3 July; accepted 1 September.

DOI: 10.24412/2221-0474-46-41-48

GSC 3989 1185 and HD142898
– New Multi-mode Low Amplitude δ Scuti Variables

Igor M. Volkov, Alexandra S. Volkova

Sternberg Astronomical Institute, Moscow University, Universitetsky Ave., 13, 119992 Moscow, Russia

A test for physical variability of stars in the immediate vicinity of two eclipsing stars showed that HD 142989, the reference star for BD –20°4369, and GSC 3989 1185, a close neighbor of V340 Lac, are low-amplitude δ Scuti variables. The first of them exhibits six pulsation modes and the second of them, two pulsation modes.

1 Introduction

Our observational program is primarily aimed at studying the internal structure of stars by measuring apsidal rotation velocities in eclipsing systems with elliptical orbits (Volkov & Volkova 2009; Volkov 2024). The program's success requires photometric measurements of the highest precision. Therefore, our ground-based measurements need careful selection of comparison stars to eliminate any additional errors that might be introduced by their physical variability. As a result and a by-product, we discover a large number of unknown low-amplitude variables.

2 Two-color diagram for δ Scuti stars

Some assistance in identifying potential pulsating stars is provided by the fact that we conduct our measurements in all $UBVRcRIcI$ bands of the Johnson–Cousins broad-band photometric system. In particular, δ Scuti stars occupy a fairly narrow region in the two-color diagrams, which prompts a more thorough examination of their variability, since pulsations often occur in multiple modes, beats can be observed, and, on some observing nights, the star shows no variations, but if the star's color indices are close to those of δ Scuti variables (type DSCT according to Samus et al. 2017), observations continue. The unreddened color indices of the DSCT stars fall within the interval $0\overset{\mathrm{m}}{.}24 < B-V < 0\overset{\mathrm{m}}{.}32$, or 7550 K $> T >$ 7100 K according to the calibration from Flower (1996). In the present study, we concentrate our attention on the regions occupied by pulsating stars in the $U-B$, $B-V$ diagram, with the interstellar absorption taken into account (see Fig. 1). The figure also shows some DSCT type variables found by us, plotted as crosses: the primary components of the eclipsing binaries V961 Cep (Volkov et al. 2010), V577 Oph (Volkov 1990; Volkov & Volkova 2010), V501 Mon (Volkova & Volkov, 2025). The prototype of DSCT stars, δ Sct, is also shown in the diagram. All stars in this diagram, with the exception of δ Sct, are subject to significant interstellar extinction.

The magnitudes of δ Sct were taken from the Sternberg Institute's catalog of bright stars (Kornilov et al. 1991) and converted to the standard Johnson system. If the interstellar extinction is known for an object, then its luminosity class can be also determined from this diagram. The interstellar extinction for δ Sct being close to zero (Gaia DR 3; Green et al. 2015), its position in the diagram unambiguously suggests the spectral type F2 II, to be compared to that in SIMBAD, F2 II–III.

3 Observations

The main part of observations for both stars were obtained at the INASAN observatory in Simeiz, on Mount Koshka, using the Zeiss-1000 telescope and an FLI16803 CCD, in the $UBVRcIc$ photometric system, and the Zeiss-600 telescope with a VersArray 512UV CCD, in the $UBVRI$ photometric system. The Zeiss-1000 and Zeiss-600 instruments are described in Nikolenko et al. (2019). The details of the instrumental $UBVRcIc$ photometric system are given in Barabanov et al. (2021). The transformation coefficients for VersArray 512UV are given in Volkova & Volkov (2026a).

Besides, HD 142989 was recently observed on five nights with the ASA AZ800 $F6.85$ 80-cm reflector of the Technology Innovation Institute Optical Ground Station (Abu Dhabi, United Arab Emirates) equipped with the QHY174M 1920 × 1200 CMOS and a green filter (4900–5800 Å) supplied with the sensor. Comparing the instrumental differences between the comparison star GSC 6199 969 and the studied stars, obtained using FLI16803 and VersArray 512UV CCDs with a QHY174M + 4900–5800 Åfilter, we find that the instrumental system is quite close to the V band. The transformation formula is as follows:

$$V_{\mathrm{Johnson}} = V_{\mathrm{inst}} - 0.137((B_{\mathrm{star}} - V_{\mathrm{star}}) - (B_{\mathrm{stand}} - V_{\mathrm{stand}})), \quad (1)$$

where the index “star” refers to the studied star and the index “stand” refers to the comparison star. The $B-V$ color indices should be determined from independent sources. The error of the transformation coefficient is ±0.015. The instrumental system is blue-shifted relative to the Johnson V band.

We processed all observations using the Maxim DL program.

4 Periodicity analysis

Data periodicity analysis was performed using our period search algorithm (Volkov 2022). First, the peak with the maximum amplitude was identified on the periodogram, see Fig. 2 for an example. Then, the initial phase and amplitude of the approximating sine curve were determined by minimizing residual deviations using the next formula:

$$V = V_{\mathrm{star}} - \Sigma_{i=1}^{N} A_i \cdot \sin\left(2\pi(\mathrm{HJD}_{\mathrm{obs}} - \mathrm{Ep}_{0i})/P_i\right), \quad (2)$$

where A_i are pulsation amplitudes, Ep_{0i} coincide with phase ϕ=0 of the corresponding sine curve, P_i are the pulsation periods, V_{star} is the corresponding magnitude from Table 1. The sinusoid with obtained parameters was subtracted from the overall data set, and the search was repeated. Thus, we identified all the dominant oscillations. In the final stages of the approximation, when all the dominant periods had been established, the pulsation parameters, including the periods, were refined using the least squares method. They are presented in Tables 2 and 3.

The pulsation amplitudes of both stars were found to be within one hundredth of a magnitude, therefore they should be attributed to the low-amplitude subtype of δ Sct stars, DSCTC according to Samus et al. (2017).

The $UBVRcRIcI$ magnitudes of both stars are given in Table 1.

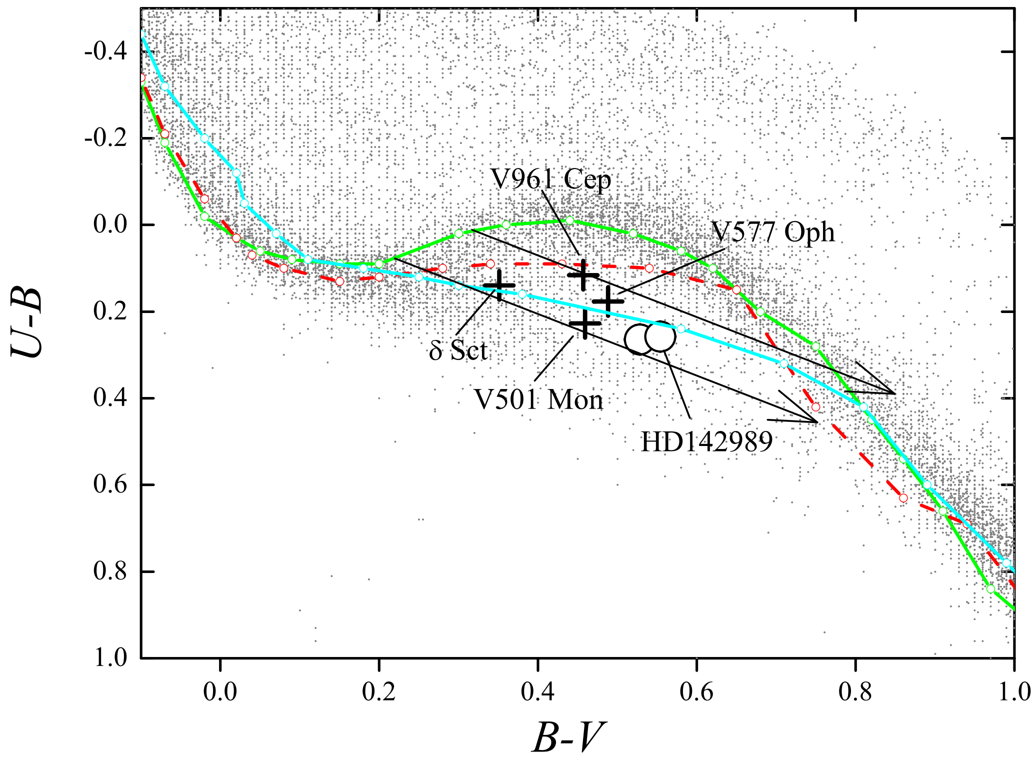

Figure 1. The $U-B$, $B-V$ diagram. Circles are DSCT stars from our study. Crosses mark some of the DSCT variables we studied previously. The colored curves indicate luminosity classes according to Straižys (1992): the green curve is for class V; the dashed red curve, class III; and the blue curve, class II. The gray dots are data from the Mermilliod et al. (1997) catalogue. The arrows of the interstellar reddening lines outline the region of DSCT stars, Sp A7–F2.

5 GSC 3989 1185

This star served as one of comparison stars in the observations of the eclipsing variable V340 Lac for more than 20 years (Volkova & Volkov 2026b). Even during the early stages of the study, it was suspected that either one of the comparison stars or V340 Lac itself was experiencing slight physical oscillations. As the observational base expanded, we discovered that it was GSC 3989 1185, situated 30″ away from V340 Lac, that was changing its brightness. Multicolor $UBVRI$ measurements of all stars in the vicinity aided in the search for the pulsating star. This star was excluded from the comparison stars, and the entire data were reprocessed. As a result, we obtained seven data sets: 188 data points in the U band; 519, in the B band; 1290, in the V band; 319, in the Rc band; 194, in the R band; 268, in the Ic band; 139, in the I band. The original data for every band can be found in the appendix to the html version of this paper as '3989 1185 $*$.txt' files. The first column of the tables indicates the Heliocentric Julian Date (HJD) of the observation, understood as the midpoint of the exposure, and the second column indicates the difference between the current star's magnitude and its average level from Table 1 in the corresponding photometric band, '$*$'.

Our observations in the V photometric band, phased with the derived periods, are displayed in Fig. 3. Pulsations with the same periods are also clearly visible in the other photometric bands, showing a noticeable tendency for the pulsation amplitude to increase with decreasing observation wavelength. This behavior is typical of DSCT variable stars.

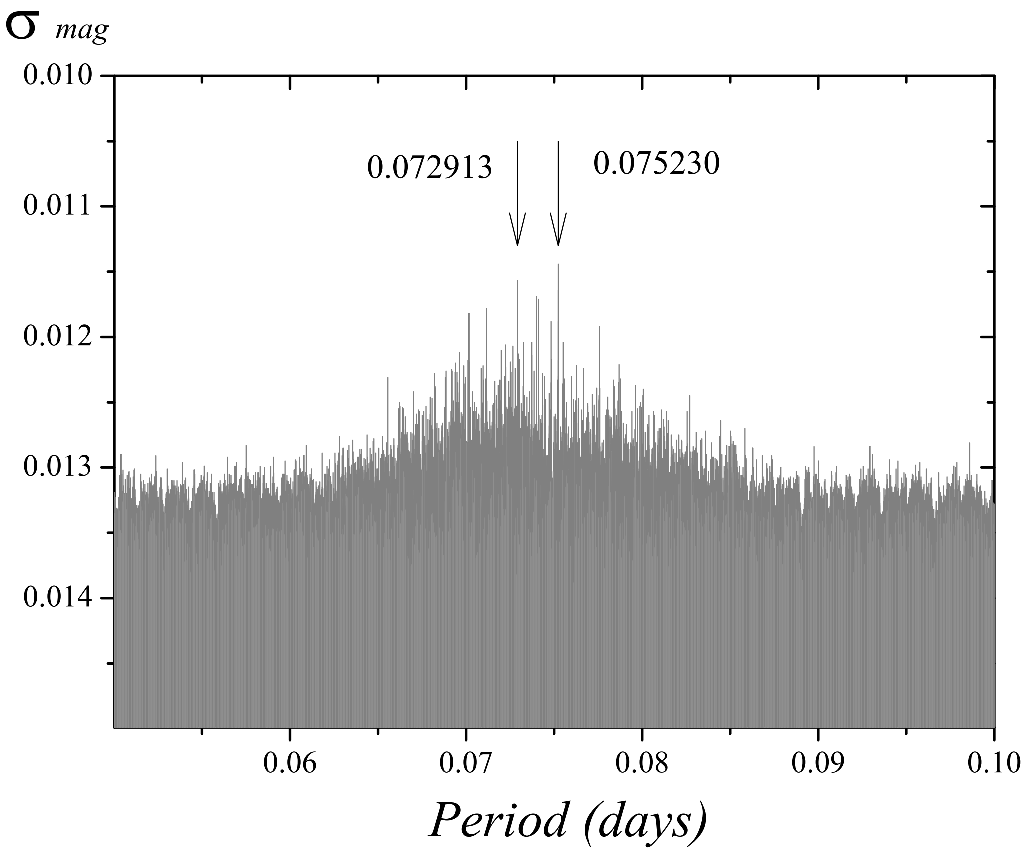

Figure 2. The periodogram of GSC 3989 1185. Arrows indicate the accepted periods from Table 2.

6 HD 142989

HD 142989 was used as a comparison star in observations of the eclipsing variable BD –20°4369. We noticed that, during synchronous observations with two telescopes, the shape of the primary minimum was distorted in the same way. Therefore, the detected systematic deviations could not be attributed to instrumental effects or atmospheric extinction. The derived $UBVRI$ magnitudes of HD 142989 showed that it fell within the instability region in the $U-B$, $B-V$ diagram, where we had already discovered a number of variable stars (see Fig. 1). Thus, we had to reprocess all our observations using a fainter comparison star GSC 6199 969 (V = 12.713). Over 14 years, we accumulated a sufficient number of observations for a detailed analysis.

To prevent saturation of the variable star measurements, the exposure duration was limited to 5–10 seconds. All data were averaged over approximately 5–20 frames to achieve an average accuracy better than $0\overset{\mathrm{m}}{.}01$. These measurements are available in an appendix to the html version of this paper as the HD 142989 V.txt file. The contents of this table is similar to the contents of the observation tables for the previous star. V magnitude to

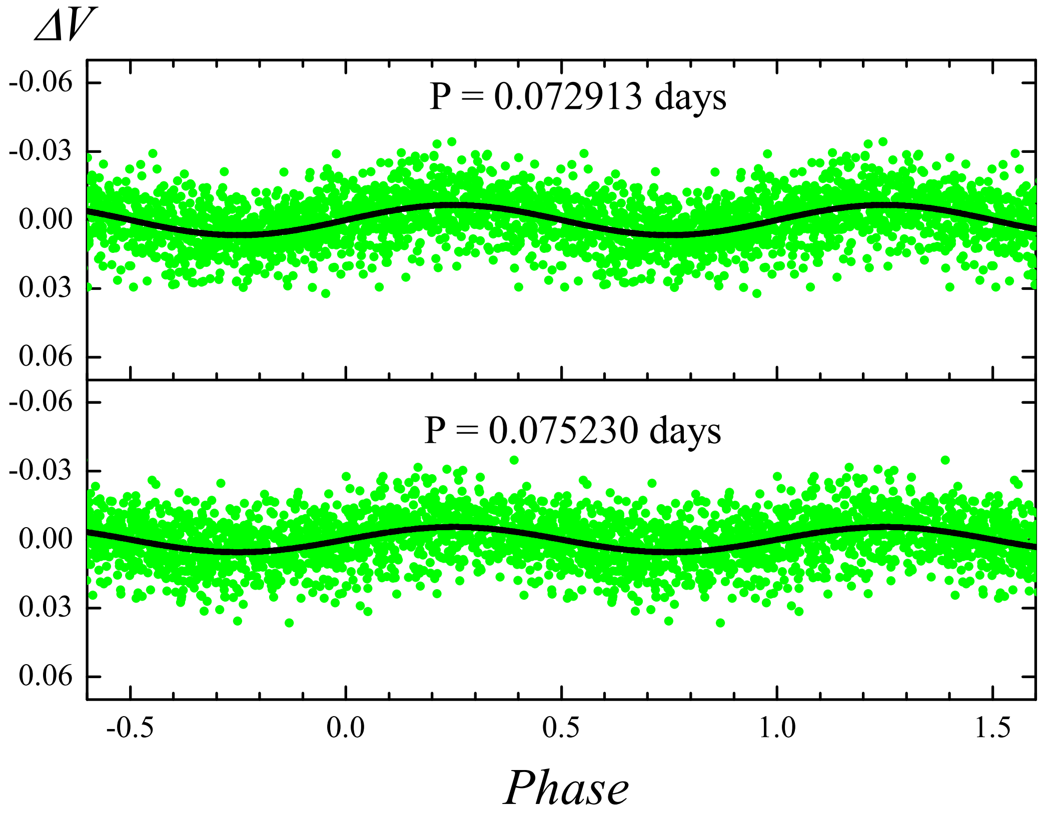

Figure 3. The light curves of GSC 3989 1185 in the V band phased with both values of the period. Pulsations with the other period were subtracted from each curve. The rms deviation of individual measurement from the mean curve is $\pm0\overset{\mathrm{m}}{.}0101$, which corresponds to the precision of our V-band observations.

be added to the differences from the second column of this table can be found in Table 1. The data were checked for outliers. If a given measurement was logically unreliable (such as clouds, a large air mass, or a sharp deterioration in the image), that data point was discarded. In total, we obtained 1162 observations in V band. Observations after JD 2461183 were acquired in Abu Dhabi.

We then tested how the identified pulsation parameters applied to individual nights. An example is shown in Fig. 4. Failure to account for any of the identified oscillations leads to increased errors on each observing night.

Our observations were separated by the following discrete intervals: a day, a year-long observation window of approximately four months, and 3.1 days. The last interval corresponds to the orbital period of the neighboring eclipsing star BD–20°4369. This is because almost all our observations were conducted during the primary minimum of this star. The required value of the period was chosen based on the minimum residual scatter of observation points. All the detected periods are significant, and excluding any of them from the analysis significantly increases the residual scatter, O–C. If the sine functions with the found periods are not subtracted, then the standard error of the scatter of observations becomes $\pm0\overset{\mathrm{m}}{.}0111$. The resulting mean error in the case when all six sine curves were extracted according to formula (2) is $\pm0\overset{\mathrm{m}}{.}0080$.

All periods from Table 3 were checked not to be aliases between each other.

It is possible that pulsations with other periods exist, but their amplitudes must be smaller than A_6 from Table 3. Our observational accuracy is no longer sufficient to detect them.

Our analysis of the TESS data (Stassun et al. 2019) revealed that they contain a pair of periods ($0\overset{d}{.}125$ and $0\overset{d}{.}109$) plus the period $0\overset{d}{.}076445$. All they are close to ours (see Table 3). We found no traces of other periods in the TESS observations. Whether this is due to the temporary disappearance of pulsations with these periods during the week of TESS observations, or maybe due to the specifics of the TESS processing, remains unclear.

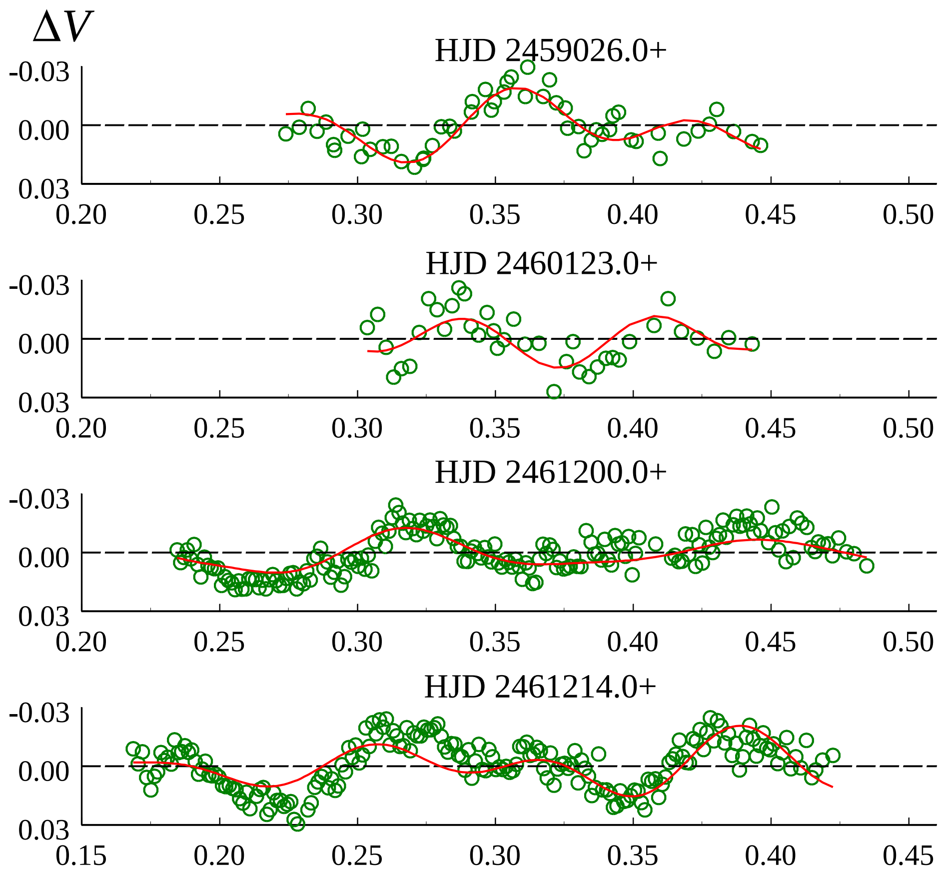

Figure 4. Four individual nights of observations (green circles). Superposition of sine curves with parameters from Table 3 (red curves). The rms deviation of individual measurement for each night, from top to bottom, is $\pm 0\overset{m}{.}0067$, $\pm 0\overset{m}{.}0098$, $\pm 0\overset{m}{.}0067$, $\pm 0\overset{m}{.}0082$.

Our multicolor observations of other stars confirm that the TESS photometric band is close to Ic (Volkov et al. 2024). The amplitude of brightness variations for $P = 0\overset{d}{.}125$ in TESS observations was derived to be $A_{\text{tess}} = 0.0027$, much lower than in the V band. This confirms the suggested DSCT variability type.

Formula (2), along with data from Table 2, helped us to reduce the scatter of our observations of the eclipsing star BD–20°4369.

7 Conclusions

Our high-precision photometric observations allowed us to detect two new DSCT variables and to analyze their periodicity. GSC 3989 1185 has two periods stable for 20 years; HD 142989 has six periods, stable for 14 years of observations. These facts are of a significant interest for the theory of stellar pulsations.

We also point out that high-precision multicolor observations are suitable for spectral classification and subsequent temperature calibration with an accuracy rivaling that of spectroscopic measurements.

The coefficient for converting instrumental magnitudes from QHY174M 1920×1200 CMOS sensor + 4900–5800 Å filter, with which we have not worked before, into the standard Johnson system was determined.

Acknowledgments: This work was carried out under the State Assignment of the Sternberg Astronomical Institute, Moscow State University.

Observations were partly conducted with the Zeiss-600 and Zeiss-1000 telescopes of the Terskol Observatory Collective Use Center of INASAN.

We express our sincere gratitude to K.S. Kravtsov for conducting remote observations at the Technology Innovation Institute Optical Ground Station in Abu Dhabi.

Thanks are due to Prof. N. Samus for helpful discussions and criticism.

This study used the SIMBAD database of the Strasbourg Astronomical Data Center (France) and the ADS bibliographic service (NASA, USA).

References:

Barabanov, S. I., Potanin, S. A., Savvin, A. D., et al. 2021, *INASAN Science Reports*, **6**, 92

Flower, P. J. 1996, *Astrophys. J.*, **469**, 355

Green, G. M., Schlafly, E. F., Finkbeiner, D. P., et al. 2015, *Astrophys. J.*, **810**, No. 1, article id. 25

Kornilov, V. G., Volkov, I. M., Zakharov, A. I., et al. 1991, Tr. Gos. Astron. Inst. **63**, 4

Mermilliod, J. C., Mermilliod, M., & Hauck, B. 1997, *Astron. & Astrophys. Suppl. Ser.*, **124**, 349

Nikolenko, I. V., Kryuchkov, S. V., Barabanov, S. I., & Volkov, I. M. 2019, *INASAN Science Reports*, **4**, 85

Samus, N. N., Kazarovets E. V., Durlevich O. V., et al. 2017, *Astron. Rep.*, **61**, No. 1, 80

Stassun, K. G., Oelkers, R. J., Paegert, M., et al. 2019, *Astron. J.*, **158**, No. 4, article id. 138

Straižys, V. 1992, Multicolor Stellar Photometry (Pachart Pub. House, Tucson)

Volkov, I. M. 1990, *IBVS*, No. 3493

Volkov, I. M. 2022, *Perem. Zvezdy*, **42**, No. 1, 1

Volkov, I. M. 2024, *Perem. Zvezdy*, **44**, No. 4, 42

Volkov, I. M. & Volkova, N. S. 2009, *Astron. Rep.*, **53**, No. 2, 136

Volkov, I. M. & Volkova, N. S. 2010, *ASP Conf. Ser.*, **435**, 323

Volkov, I. M., Volkova, A. S., & Bagaev, L. A. 2024, *Astron. Rep.*, **68**, No. 9, 886

Volkov, I. M., Volkova, N. S., & Chochol, D. 2010, *Astron. Rep.*, **54**, No. 5, 418

Volkova, A. S. & Volkov, I. M. 2025, *Astron. Rep.*, **69**, No. 6, 480

Volkova, A. S. & Volkov, I. M. 2026a, *Astrophys. Bull.*, **81**, No. 3, 360

Volkova, A. S. & Volkov, I. M. 2026b, *Astron. Rep.*, **70**, No. 5, 547

Table 1: Mean magnitudes of the stars

Star	V	$U-B$	$B-V$	$V-R_C$	$V-R$	R_C-I_C	$R-I$	$E(B-V)$	Sp
GSC 3989 1185	13.216	0.258	0.554	0.329	0.489	0.389	0.431	0.295	A9 V
	±0.007	±0.011	±0.008	±0.016	±0.016	±0.018	±0.009	±0.020	
HD142989	9.090	0.264	0.528	0.305	0.455	0.287	0.302	0.280	A9 V
	±0.004	±0.023	±0.007	±0.021	±0.018	±0.044	±0.043	±0.020	

Table 2: Pulsation parameters for GSC 3989 1185

i	Ep_{0i} 2,453,305+	P_i days	A_i V mag
1	0.2583 ±0.0002	0.07291306 ± 0.00000003	0.0066 ±0.0002
2	0.2590 ±0.0002	0.07523032 ±0.00000003	0.0055 ±0.0002

Table 3: Pulsation parameters for HD 142989

i	Ep_{0i} 2,460,775+	P_i days	A_i V mag
1	0.4830 ±0.0003	0.12439667 ± 0.00000015	0.0070 ±0.0002
2	0.5148 ±0.0012	0.06753583 ±0.00000006	0.0048 ±0.0001
3	0.6589 ±0.0002	0.10837759 ±0.00000005	0.0043 ±0.0002
4	0.5048 ±0.0002	0.06314659 ±0.00000005	0.0040 ±0.0002
5	0.5231 ±0.0010	0.08100005 ±0.00000005	0.0026 ±0.0002
6	0.5358 ±0.0002	0.07644490 ±0.00000008	0.0022 ±0.0006